International Journal of Adhesion & Adhesives 31 (2011) 331–337

Contents lists available at ScienceDirect

International Journal of Adhesion & Adhesives

journal homepage: www.elsevier.com/locate/ijadhadh

Numerical stress analysis of carbon-fibre-reinforced epoxy composite single-lap joints

F.L. Ribeiro [a], L. Borges [a], J.R.M. d'Almeida [b,*]

[a] Mechanical Department, Universidade Federal do Rio de Janeiro, Centro de Tecnologia, Bl. G, Cidade Universitária, Rio de Janeiro-RJ, Brazil
[b] Materials Engineering Department, Pontifícia Universidade Católica do Rio de Janeiro, Rua Marquês de São Vicente, 225, Gávea 22451-900, Rio de Janeiro, RJ, Brazil

ARTICLE INFO

Available online 4 March 2011

Keywords:
Single-lap joints
Composites
Numerical analysis
FEM

ABSTRACT

A numerical strategy based on a finite element method is developed in order to model the stress distribution in single-lap adhesive joints. The joints were manufactured from unidirectional carbon-fibre-reinforced epoxy composites joined by an epoxy adhesive layer. Experimental parameters are used as a reference to allow for the numerical validation of the proposed analysis. Additionally, joints with different types of defects in the lap region were modelled with both two-dimensional and three-dimensional finite elements. The models include defects that vary in format (straight or circular) and position (centred or dispersed). The influenced spew fillets in the adhesive layer were also examined. Although the computational cost is higher, the results of the three-dimensional model are more compatible with the experimental results than those of the two-dimensional model. The effect of defects in the joints was adequately modelled, and the proposed methodology can be used to accurately assess the integrity of the joints since the defect has been successfully detected.

1. Introduction

As the use of composite materials has gained great popularity in the past decades, with it arose the need to join the components and structures assembled with these materials. Traditional methods of joining, such as riveting and screwing, became the first choice due to their relatively low cost and ease of assembly. However, as is already widely known, even when such joints are used with traditional materials, high stress concentrations can develop at the point of joining, and the joint can be brought to failure at far lower stress levels than expected. Besides, non-metallic composites are not able to accommodate plastic deformations, and therefore, stress concentration can lead to premature failure of the bonded joint.

Consequently, the use of adhesives for joining composite structures became a common practise. Adhesives present several advantages over the traditional joining methods such as prevention of high stress concentrations and contribution to a much more uniform stress distribution between the components of a structure [1].

Among the most frequently used and most thoroughly studied adhesive joints are the lap joints [1,2]. In single-lap joint configuration (Fig. 1), two sheets overlap in such way that an in-plane tensile load applied at the sheets produce shear and peel stresses in the adhesive as well as on the faces of the adherends [2]. Single-lap joints are easily assembled but care has to be taken regarding the excess of adhesive that flows out from the lap area since the presence of spew fillets can greatly affect the stress distribution at the joints. In fact, surrounding the edge between the adhesive and the adherend can promote a more uniform stress and strain distribution. Therefore, the presence of spew fillets can increase the strength of the lap joint [3].

Although there are ongoing efforts to develop analytical and numerical models for suitably describing the stress distribution of single-lap joints [4–11], numerical stress analysis methods that include the effects of defects at the bonded area are still scarce and the defects are usually modelled as strip, delamination-like, defects [12,13]. An extensive review and comparative study of the different approaches adopted to study adhesively bonded joints is presented in da Silva et al. [10,11].

Besides strip defects, one can also expect that void-like defects, arising both from volatile by-products that can evolve during the adhesive curing or from entrapped air bubbles [14] can be found at an adhesive joint. The lack of appropriate methods for this type of defects has motivated this study, where the stress distribution of single-lap joints with round defects at the bonded area is modelled. In order to validate the model, joints without defects were also modelled, and the results of the numerical analysis were compared with previously published experimental results [15,16].

2. Composite joints

The joints were manufactured using a unidirectional carbon-fibre-reinforced epoxy composite with 0.55 volume fraction of

* Corresponding author. Tel.: +5521 35271234; fax: +5521 35271236.
E-mail address: dalmeida@puc-rio.br (J.R.M. d'Almeida).

0143-7496/$ - see front matter © 2011 Elsevier Ltd. All rights reserved.
doi:10.1016/j.ijadhadh.2011.01.008

fibres as the adherend. Single-lap joints 80 mm long and 25.4 mm wide were fabricated with an overlap length of 25.4 mm. The epoxy system used as the adhesive was composed of the epoxy monomer diglycidyl ether of bisphenol-A (DGEBA) and the triethylene tetramine (TETA) hardener. The hardener to epoxy ratio was 13 parts in weight of hardener to 100 parts in weight of resin. This ratio corresponds to the stoichiometric ratio of this epoxy system.

The adhesive was applied using the brushing technique, and the curing of the joint was performed at room temperature, 23 ± 3 °C, for 24 h, while maintaining the joint area under a pressure of 2.7 kPa. Defects were introduced at the centre of the joints using discs of poly(tetrafluoroethylene) because this material does not adhere to epoxy adhesives. More details regarding the joint manufacturing process, as well as the experimental procedures used to test and characterize the joints, can be found elsewhere [15,16]. Table 1 lists the basic mechanical properties of the unidirectional composite used as adherend and the epoxy used as adhesive [15–17].

3. Numerical modelling

The numerical analysis was performed using the finite element method (FEM) package ABAQUS®. At first, the joint without defects was modelled using a 2D approach. Then, the analysis of the same joint was carried out with a 3D model, which requires more processing time, but simulates the actual behaviour of the joint more accurately. The analysis of the joint without defects was used as a verification step in calibrating the numerical analysis with the experimental results. Subsequently, the joints with defects were also analysed by both 2D and 3D models.

Due to the simple geometry of single-lap joint, the strategy adopted to model its behaviour follows the main steps available in the FEM package [18]:

- *Parts:* The lower and upper adherend strips and the adhesive layer were geometrically generated. The shell shape was used for three parts.

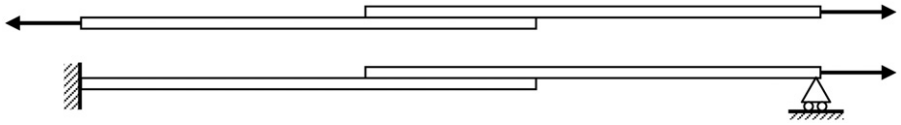

Fig. 1. Single-lap joint assembly and loading direction (top) and associated FEM model (bottom).

Table 1
Tensile mechanical properties of the materials used.

	Tensile strength (MPa)	Elastic modulus (GPa)	Deformation at rupture (%)
Adherend (carbon fibre composite in longitudinal direction)	983 ± 38	86.9 ± 4.2	1.02 ± 0.02
Adhesive (epoxy resin)	80.0 ± 4.7	3.84 ± 0.6	3.3 ± 0.2

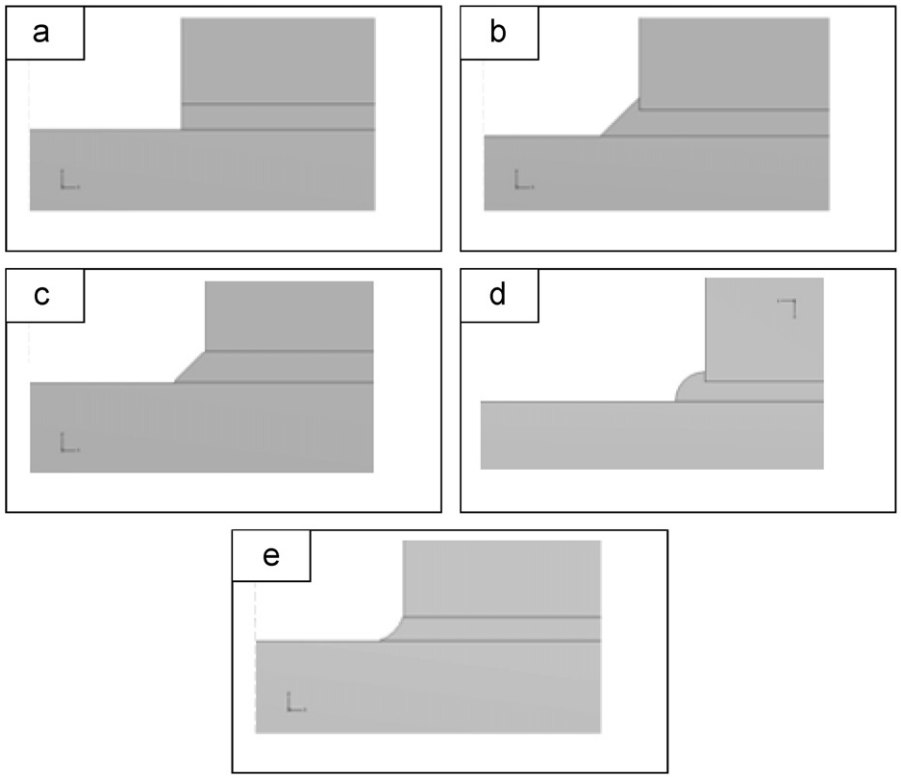

Fig. 2. Configurations of free edges of the lap joints: (a) straight edge, (b) 45° standard chamfer [1], (c) 45° chamfer, (d) standard spew fillet [13] and (e) spew fillet with adhesive contraction.

- *Assembly*: Three independent parts were merged. The joint was composed of two materials, composite and adhesive, without contact boundaries between them, simulating a co-curing joint.

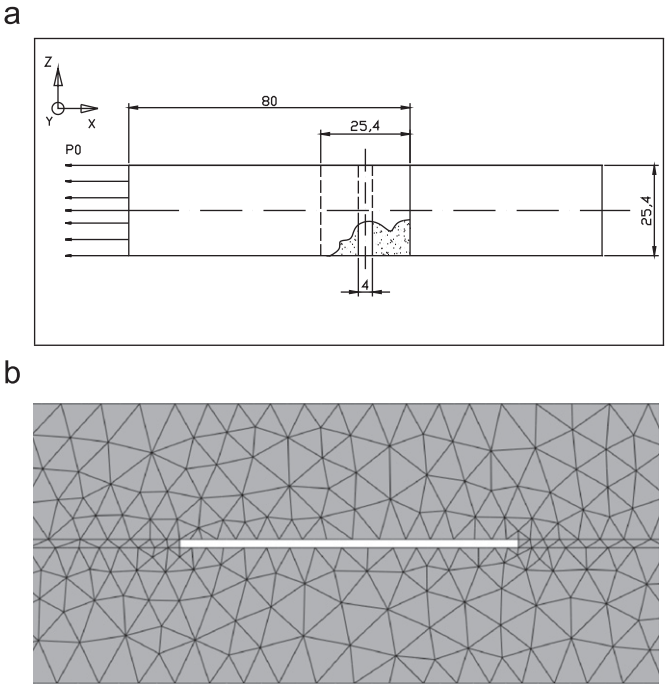

Fig. 3. Schematic representation of 2D model of the defects. Symmetrical model (a) central position of the strip defect and (b) mesh generated close to the defect position. All dimensions are quoted in mm.

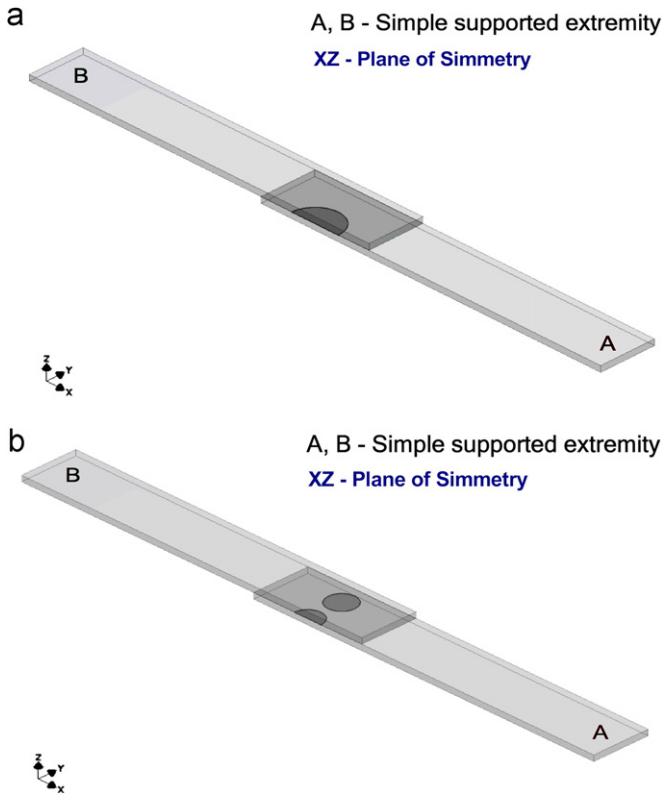

Fig. 4. Schematic representation of the joints with defects, 3D analysis: (a) central defect and (b) edge defects. The defects are symmetrical regarding to XZ-plan.

- *Mesh:* To determine the most appropriate mesh element for the problem, several elements were tested. For 2D analysis, planar elements, in-plane stress condition were used. After preliminary tests, a triangular element was chosen, and a higher number of elements were used near the edge of the adhesion line, where higher stress gradients are present. For 3D analysis, a four node tetrahedral linear element was used to model the substrates. The adhesive was modelled using eight-node hexahedral linear elements. All parts are assumed to be constituted of an elastic linear material. In fact, the epoxy resin used as adhesive has a non-linear behaviour near its fracture stress [19]. However, when confined to a very small layer between adherends, epoxies show a linear elastic behaviour up to rupture [20].
- *Step:* At this point, loading and boundary condition steps were defined. Namely, one of the extremities of the joint, at the area under the grip of the tensile test machine, has the restrictions of a cantilever beam, and the other extremity acts as a simple supported beam. The loading was defined by an axial force applied at the simple supported extremity (Fig. 1). Furthermore, the parameters for controlling the non-linear geometrical effects were established.

The geometry of the edges at the lap region used to model the 2D joints is shown in Fig. 2. In addition to the straight edge obtained when the excess of adhesive is removed during the joint manufacturing process, the presence of chamfers and spew fillets

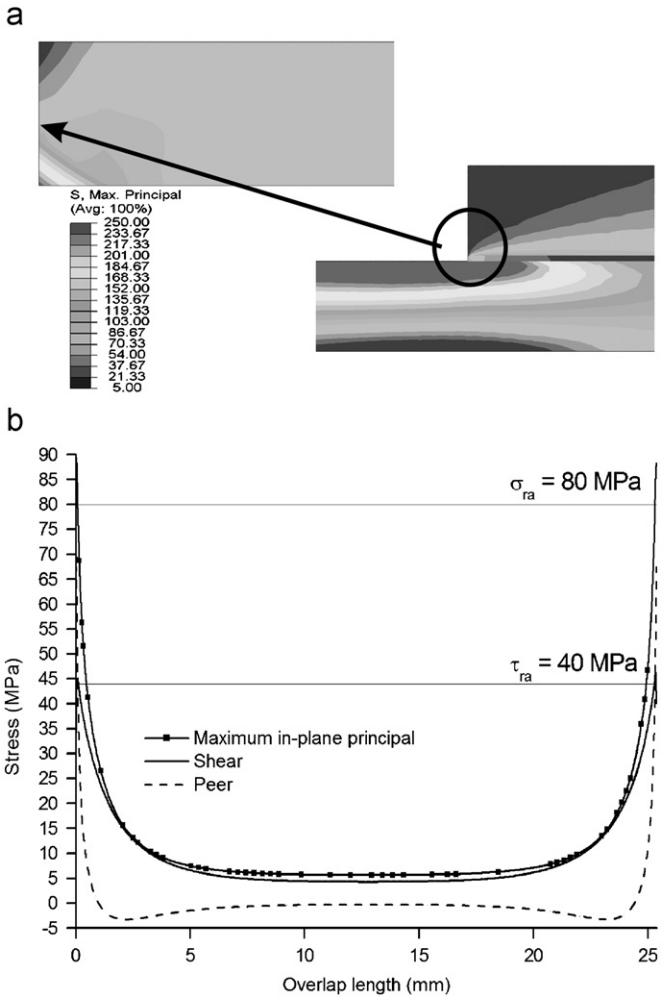

Fig. 5. (a) Maximum in-plane principal stress distribution on adhesive 2D single-lap joint without defects and (b) Peel, shear and maximum in-plane principal stress distributions on adhesive layer.

was considered. In both these cases, two configurations were used, and the choice was based either on the literature [1,21] or on the analysis performed during the development of this work. For the 3D model, only straight edges were analysed.

The strategy used to model the joints with defects followed the same steps listed above with the exception of logical introduction of the defects. For 2D model, the defect introduced was restricted by the 2D configuration to a rectilinear discontinuity along the 25.4 mm width of the joint and encompassing the entire thickness of the adhesive layer. This same approach was used by Moura et al. [13]. The defect was placed in the middle of the lap region and was 4 mm wide. Fig. 3 shows the localisation of the defect and, also, presents the mesh used to model its effect on the behaviour of the joint.

For the 3D model, circular defects can be introduced. At first, a circular defect, 11 mm in diameter, was placed at the centre of the lap region. The FEM mesh used was generated using a four node tetrahedral linear element. To verify the effect of localisation of the defect and the number of defects on the lap strength, a second joint was modelled with three defects, 6.3 mm in diameter, placed near the edge of the lap joint. The two configurations of joints with defects are depicted in Fig. 4. It is worth mentioning that the symmetry of this system allows us to perform the analysis on only half of the joint.

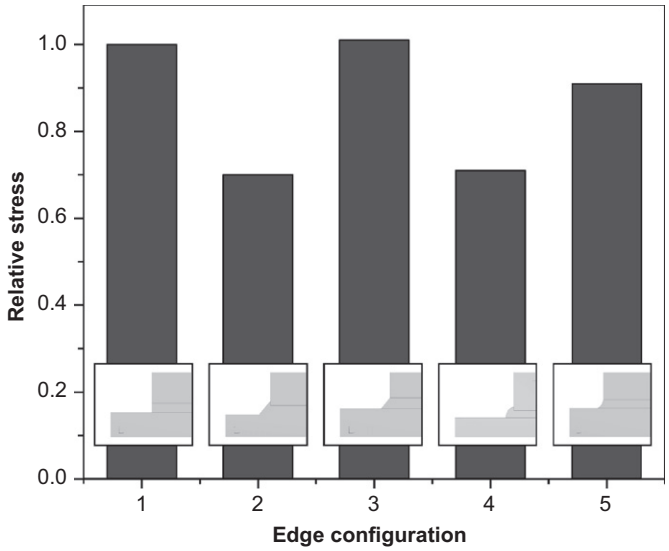

Fig. 6. Effect of chamfers and spew fillets on the maximum tensile stress at the adhesive layer. Relative stress is the stress found for each spew/chamfer configuration divided by the stress found when a straight edge joint was used.

4. Results

4.1. Joints without defects—2D model

The maximum in-plane principal stress distribution obtained from the 2D model of the joints without defects or spew fillets is shown in Fig. 5a. The caption refers to the stresses in the adhesive region highlighted on the figure. The stress distribution in the adhesive is depicted in the Fig. 5b, where an increase of the stresses at the edge of the joint is observed, in accordance with the behaviour described in the literature [5–7,10,11,21,22]. In addition, as shown in Fig. 5b, the maximum in-plane principal stress at the adhesive layer (75 MPa), near the edges, is in good correlation with the adhesive failure normal stress of 80 MPa [16,17]. This stress distribution was obtained when non-linear geometrical effects were controlled, and a 2D element in the plane stress state was used. The non-linear geometrical effects were also previously used by other authors [13,23].

It is clear that the stress concentration at the edge of the lap joint (maximum in-plane principal stress of approximately 90 MPa) is an inadequacy of the FEM to deal with stress singularities points, even when adaptive meshes strategies are considered. In spite of this numerical drawback, the analysis is useful to identify the critical points. Far from the edges the results compare well with the results obtained by the authors above mentioned.

Moreover, it is widely known that in the vicinity of the singularities points prevails a three-dimensional stress state. Therefore, it is easy to foresee that a two-dimensional model is unsuitable to represent these local stresses.

The effect of the presence of chamfers and spew fillets on the maximum normal stress acting at the adhesive layer can be seen in Fig. 6, where the stress found for each spew/chamfer configuration was divided by the stress obtained when a straight edge

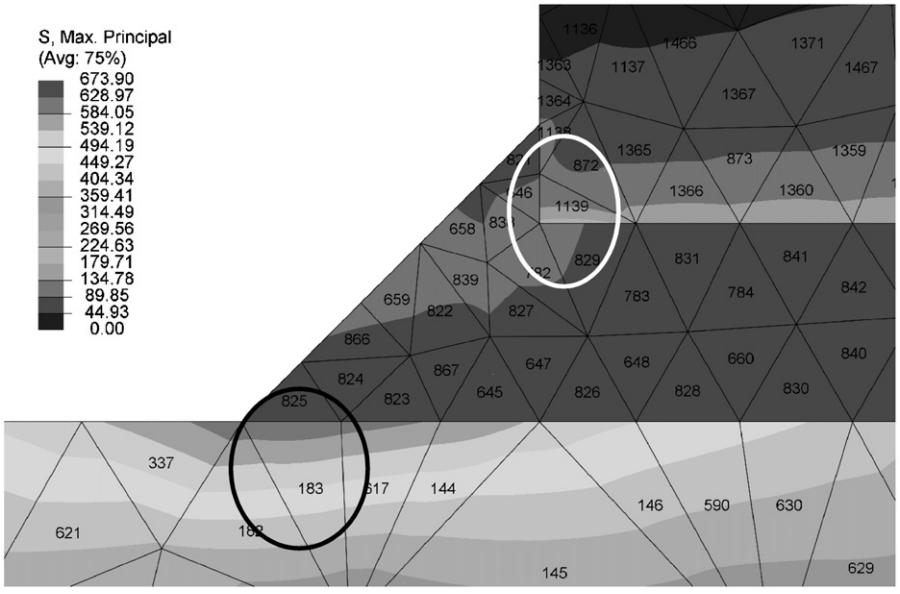

Fig. 7. Maximum tensile stress in the adherends at the edge of the lap. Example shown is for the standard chamfer edge.

joint was used. As expected from the data found in the literature, the standard chamfer reduces the stress concentration [1] and thus, the maximum stress at the adhesive layer. The same reduction of the stress concentration occurred when a protruding spew fillet was used [21]. The configuration with a straight 45° chamfer, without any overlapping of the adherent by the adhesive, did not alter the stress distribution at the joint and spew, taking into account resin contraction, had only a minor effect on the maximum tensile stress acting on the adhesive layer.

Table 2
2D analysis of the lap-joint using Tsai—Wu criterion.

Element number	σ_{11} (MPa)	σ_{22} (MPa)	σ_{12} (MPa)	Tsai—Wu index	Result
182	421	25	27	0.6	**Did not fail**
183	493	37	31	1.1	**Failed**
337	517	6	25	0.2	**Did not fail**
1139	106	59	49	2,4	**Failed**

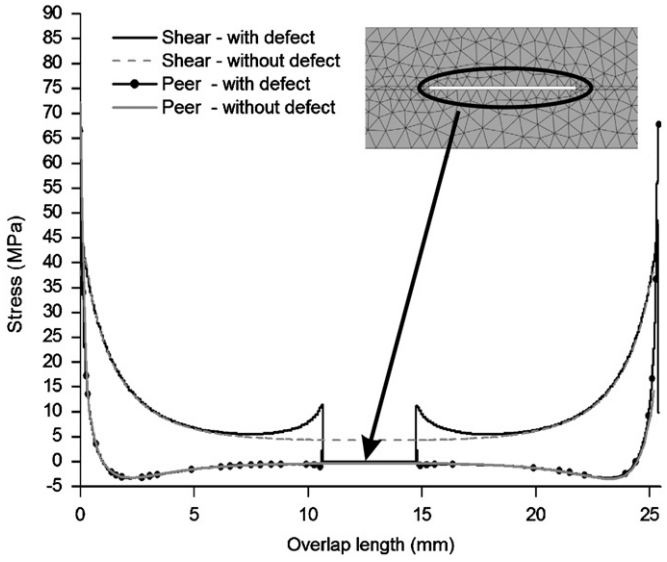

Fig. 8. Shear and peel stresses at the adhesive in the presence of a central strip defect: 2D model.

Fig. 7 shows, in detail, the stress distribution at the lap edges when the average experimental breaking load of these joints (i.e., P=6.1 kN [15]) was used in the 2D model. With these values, and using the Tsai–Wu failure criterion, it was found that failure starts near the edges of the joints [24], namely the region near elements 183 and 1139, highlighted in Fig. 7. Table 2 shows the results of Tsai–Wu analysis for some of the elements of the 2D mesh. These results show failure at the adhesive layer and also at the adherend. However, experimental evidences show that the failure of these joints was governed by adhesive rupture at the adhesive/adherend interface and cohesive failure of the adhesive layer [15].

4.2. Joints without defects—3D model

The stress distribution obtained using a 3D model of the joints without defects showed a close agreement with the results obtained from the 2D model. Once again, the control of non-linear geometrical effects had to be employed. Of course, the use of a 3D model increases the computational processing time up to 50% and, therefore, in case of the joints without defects, there was no advantage of using 3D model. Its use, however, is essential to describe the joints with defects, as will be discussed later. Therefore, 3D modelling of the joints without defects can be regarded as a way to adjust the output of the model in order to give reliable data when the defects are included.

4.3. Joints with defects—2D model

The results obtained when defects were introduced at the joints and modelled with a 2D approach are summarised in Fig. 8, where both peel and shear stresses are shown. Qualitatively, the results show that only in the vicinity of the defect a perturbation of the stress distribution occurred, in comparison to the stress distribution of the joint without defects (Fig. 8). Higher stresses at the adhesive layer still occurred at the edge of the lap region. Similar results are also described in the literature [13,25].

The absolute numerical results obtained with this model did not, however, match the experimental ones. In fact, the maximum peel stress at the joint is about 65 MPa when the joint failure load is applied. This stress is, however, smaller than the tensile strength of the epoxy adhesive (80 MPa [17]).

Nevertheless, when the maximum principal stress is considered, as well as in the joints without defects, the maximum stress

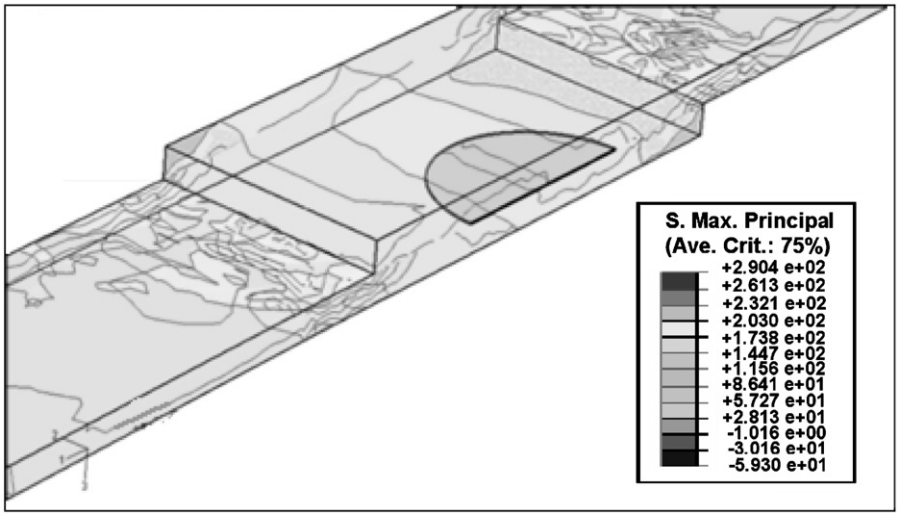

Fig. 9. 3D model—maximum principal stress in the presence of a central defect.

found by the model is roughly 75 MPa, close to the limit stress of 80 MPa, experimentally obtained for the epoxy resin.

4.4. Joints with defects—3D model

At first, the ability of adopted 3D model for describing the experimental behaviour of the joints with defects was checked. By analysing Fig. 9, it is possible to conclude that the introduction of a central defect generates an expected stress concentration at the joint. Macroscopically, this was observed by a decrease of the load bearing capacity of the joint from 6.1 to 4.7 kN [15]. In other words, when lower experimental load obtained for the joint and a central defect [15] was imposed on the 3D model of the joint a maximum adhesive stress was achieved, leading to joint failure. However, the obtained results showed that the maximum stress is still occurring at the lap edge. This result could be anticipated since the central region of a lap joint is lightly stressed when compared to the stress acting at its edges, as shown in Fig. 5b, and as described in the literature [10,26].

As described on the above paragraph, good agreement between the numerical 3D model of the joint with defects and the experimental results allowed us to use this model to simulate a joint with several defects at the bond area. The results for the lap-joint with several defects are shown in Fig. 10. Although the defect area was maintained constant with respect to the area occupied when only a central defect was used, it can be seen that a sharp reduction of the external load occurred, and caused failure of the joint. The observed load decrease can be attributed to the higher stress gradient at the lap edge, caused by the stress concentration due to the defects, as shown in Fig. 11. Since the load values causing the failure of the joints without defects and with a central defect were checked against the experimentally obtained rupture loads [15], the 3D model here presented can be used to infer the average failure stress of a lap joint once a defect is detected.

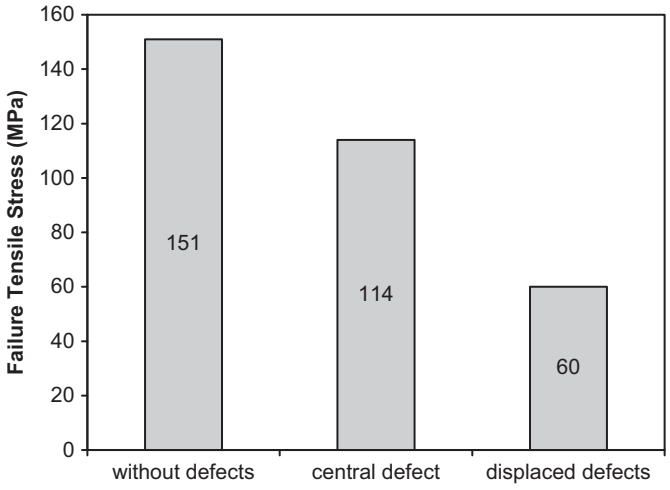

Fig. 10. 3D model—tensile stress to cause failure of the joints without defects (1), with a central defect (2) and with displaced defects (3).

5. Conclusions

The numerical analysis performed underlined the importance of controlling the region of the joint edge, since spew fillets or chamfers can significantly affect the stress in this region. From a practical point of view, the commonly observed configuration of a spew with resin contraction does not alter the stress at the adhesive layer, meaning that this spew fillet need not be removed, which saves time during joint production.

For the joints without defect, both 2D and 3D models showed a close agreement with the experimental results. As expected, the 3D model increased the computational processing time and, therefore, presents no advantages over the 2D model when joints without defects are considered. 3D modelling of these joints serves, however, to adjust the model output, giving more reliable data when defects are introduced.

When joints with defects were analysed, the 2D model failed to reproduce the experimental values. This behaviour was attributed to the geometrical constraint imposed on the defect by 2D models, where only strip like defects can be considered, while real joints could have circular defects.

The 3D model was able to reproduce the predicted adhesive failure load with confidence when a central circular defect was introduced at the joint. The stress distribution for these joints showed two regions of stress increase. One associated with the defect and the other at the lap edge. The latter presented the higher stress values, indicating that for a central defect, joint edges remain the main point of concern for single-lap joints. The introduction of small defects placed closer to the joint edge caused a significant reduction in the joint failure stress, corroborating the former statement.

Since the 3D model of the joint with a central defect was checked against experimental data, and the model of the joints

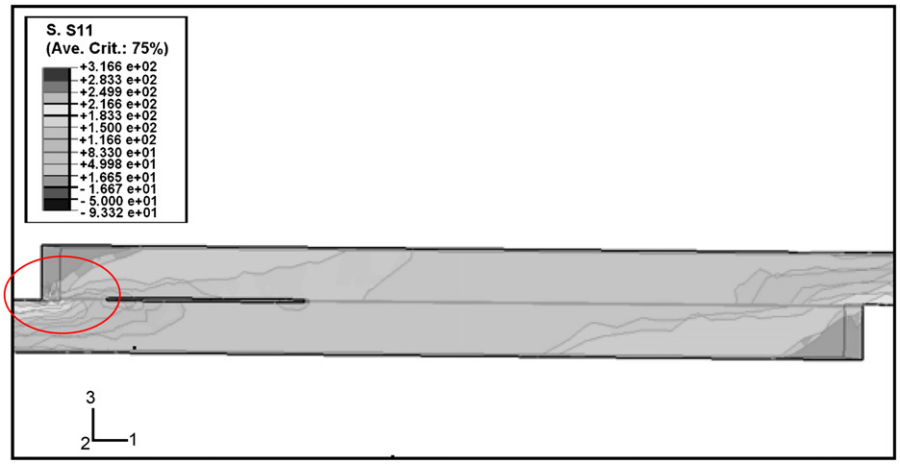

Fig. 11. Peel stress distribution of the lap joint with displaced defects.

with defects placed near the joint edge qualitatively described the predicted behaviour, it is postulated that the 3D model developed in this work can be used to predict the average failure stress of lap joints once a defect is detected at the bond area.

Acknowledgements

The authors would like to acknowledge the financial support from the Brazilian Agency CNPq and CAPES.

References

[1] Pocius AV. Adhesion and adhesives technology: an introduction. 1st ed. Cincinnati: Hanser Gardner Publications; 1997.
[2] Kinloch AJ. Adhesion and adhesives science and technology. London: Chapman and Hall; 1987.
[3] Adams RD, Harris JA. The influence of local geometry on the strength of adhesive joints. Int J Adhes Adhes 1987;7:69–80.
[4] Goland M, Reissner E. The stresses in cement joints. ASME J Appl Mech 1944;1:A17–27.
[5] Hart-Smith JL. In: Reinhart TJ, editor. Engineered materials handbook-composites, vol. 1. Metals Park, OH: ASM International; 1987. p. 479–95.
[6] Wang CH, Rose LRF. Determination of triaxial stresses in bonded joints. Int J Adhes Adhes 1997;17:17–25.
[7] Her S-C. Stress analysis of adhesively-bonded lap joints. Compd Struct 1999;47:673–8.
[8] Lang TP, Mallick PK. The effect of recessing on the stresses in adhesively bonded single-lap joints. Int J Adhes Adhes 1999;19:257–71.
[9] Kim K-S, Yi Y-M, Cho G-R, Kim C-G. Failure prediction and strength improvement of unidirectional composite single lap bonded joints. Compd Struct 2008;82:513–20.
[10] da Silva LFM, das Neves PJC, Adams RD, Spelt JK. Analytical models of adhesively bonded joints—Part I: literature survey. Int J Adhes Adhes 2009; 319–30.
[11] da Silva LFM, das Neves PJC, Adams RD, Wang A, Spelt JK. Analytical models of adhesively bonded joints—Part II: comparative study. Int J Adhes Adhes 2009;29:331–41.
[12] Olia M, Rossetos JN. Analysis of adhesively bonded joints with gaps subjected to bending. Int J Solids Struct 1996;33:2681–93.
[13] de Moura MFSF, Daniaud R, Magalhães AG. Simulation of mechanical behaviour of composite bonded joints containing strip defects. Int J Adhes Adhes 2006;26:464–73.
[14] Paciornik S, d'Almeida JRM. Measurement of void content and distribution in composite materials through digital microscopy. J Comp Mater 2009; 101–12.
[15] Berry NG, d'Almeida JRM. The influence of circular centered defects on the performance of carbon–epoxy single lap joints. Polym Test 2002;21:373–9.
[16] Berry NG. Evaluation of the influence of defects on the mechanical behavior of adhesively bonded composites, MSc thesis. Pontifícia Universidade Católica do Rio de Janeiro; 1998 [in Portuguese].
[17] d'Almeida JRM, Monteiro SN. The influence of the amount of hardener on the tensile mechanical behavior of an epoxy system. Polym Adv Technol 1998;9: 216–21.
[18] Abaqus/CAE User's Manual.
[19] Graça MLA, d'Almeida JRM, Darwish FAI. Fracture mechanisms in epoxy resin. J Braz Soc Mech Sci 1989;11:133–46.
[20] Asp LE, Berglund LA, Gudmundson P. Effects of a composite-like stress state on the fracture of epoxies. Compd Sci Technol 1995;53:27–37.
[21] Kim K-S, Yoo JS, Yi Y-M, Kim C-G. Failure mode strength of uni-directional composite single-lap bonded joints with different bonding methods. Compd Struct 2006;72:477–85.
[22] Quaresmin M, Ricotta M. Stress intensity factor and strain energy release rates in single lap bonded joints in composite materials. Compd Sci Technol 2006;66:647–56.
[23] Andreassi L, Baudille R, Biancolini ME. Spew formation in a single lap joint. Int J Adhes Adhes 2007;27:458–68.
[24] Ribeiro FL. Stress numerical analysis of single lap adhesive composite joints, MSc dissertation. Universidade Federal do Rio de Janeiro; 2007 [in Portuguese].
[25] Gonçalves JPM, de Moura MFSF, Magalhães AG, de Castro PMST, Application of interface finite elements on three-dimensional progressive failure analysis of adhesive joints. Fatigue Fract Eng Mater Struct 2003; 26:477-486.
[26] Panigrahi SK. Damage analyses of adhesively bonded bingle lap joints due to delaminated FRP composite adherends. Appl Compd Mater 2009;16:211–23.